FAST ESTIMATION OF SINGLE SCATTERING PROJECTIONS: A SIMULATION CASE IN CONE-BEAM CT

R. Thierry [a], A. Miceli[ab] , J. Hofmann [a], A. Flisch [a]

[a]*Empa – Swiss Federal Laboratories for Materials Testing and Research,*
Electronics/Metrology/X-ray Imaging Laboratory
Ueberlandstrasse 129, Duebendorf 8600, Switzerland

[b]*Università di Bologna, Department of Physics, C.*
Berti Pichat 6/2 Bologna 40127, Italy

ABSTRACT

A fast simulation of the single scattering intensity in cone beam geometry is presented. For that purpose a deterministic approach is coupled with the Forced Detection technique, a method classically employed to achieve a basic speed up of Monte Carlo simulations. The residual noisy signal is subsequently deconvoluted with the iterative Richardson-Lucy (RL) algorithm. The RL fit is performed separately on each detector plane and thereafter in the angular direction. By doing so we make use of the a priori smoothness of scatter distributions both in the detector plane and in the angular dimension. The proposed method has been validated on a CAD model of a motorcycle engine cylinder. We show that, when compared to the full deterministic simulation, the presented scatter simulation presents an acceleration of more than four orders of magnitude. The proposed method is especially robust to low number of forced detectors and gives the best results after one iteration of the RL. This versatile simulator makes it feasible to compute rapidly a complete set of cone-beam scatter projections in few decades of minutes on a single computer. Therefore it represents a potential method for fast Compton artefact reduction.

Keywords: Computed Tomography; Deterministic Simulation; Single Scattering; Forced Detection; Cone beam;

1. INTRODUCTION

Scattered photons and beam hardening are the dominant effects in Cone-beam CT systems that lead to significant degradation of the image quality. Both effects contribute to strong cupping artefacts and cause streaks to appear between dense parts in the reconstructed image [1]. The geometry of the setup, the x-ray spectrum and the nature of the object (material, thickness, geometry) all play a key role in the amount of x-ray scattering generated by the object [2, 3]. The scatter-to-primary ratio (SPR) is known to be an increasing function of the object thickness, the object field size and the atomic number [2], thus X-ray radiographies of automotive cast-parts frequently generate images with high SPR. For instance, 200 keV photons projected on a 2 cm thick iron plate generate a SPR of more than 100 % in individual detector pixels in the shadow of the object [4].

With the progress in computation capabilities, elaborated software techniques have become the leading edge in scattering reduction techniques. Recent publications showed that they provide the most accurate and advantageous solution [5, 6]. They rely on MC computer simulations, numerical approximations of the scattering functions, or by combining the two in so-called hybrid methods. Some authors adapted a MC simulator with the possibility to handle the geometric complexity of CAD models [7], or developed accelerated in-house MC with techniques such as the Forced Detection (FD) [8]. Because single scattering (i.e photons undergoing strictly one interaction with the object) often constitutes the prevailing part of the scattering signal, deterministic methods have alternatively been proposed to assess the scattering in radiographic [4] and in tomographic images [5]. They present the advantage to provide a noise-free scattering estimation. Because the required computing time is only slightly lower then classical MC, they still require a significant acceleration for their use in CT image correction. As stand-alone methods they are particularly relevant for objects generating predominantly single scattering. This method must be embedded in an hybrid method when multiple scattering can not be neglected, wherein the latter is generally handled with a fast numerical method, for instance with a rapid Monte Carlo technique [5,6].

This paper focus on the acceleration of the deterministic simulation of single scattering. A presentation of the method itself is given in paragraph 2. Material and methods of analysis are described in paragraph 3 and results are presented in paragraph 4, with a focus on parameter estimation and the acceleration factors.

2. METHOD

2.1. DETERMINISTIC SIMULATION OF SINGLE SCATTERING COUPLED WITH THE FORCED DETECTION METHOD

The deterministic simulation of the single scattering can be viewed as the numerical evaluation of an integral over the volume defined by the active voxels *v* (i.e all voxels that represent a part of the material) and the energy spectrum of the x-ray

tube. For projection angle θ and for each detector element with index (i,j), this integral can be expressed in a short form as :

$$I_s^1(i,j,\theta) = \iint_{v\in V,E} \varepsilon_{\det}(E,\alpha,Z_{\det}).dN_v(E).(dp_{Ra}(E)+dp_{Co}(E))dEdv \quad (1)$$

where $\varepsilon_{\det}(E,\alpha,Z_{\det})$ models the detector response as a function of the energy E, the angle α between the photon and the normal vector of the detector plane, and $Z_{\det}$ the atomic number of the detector. The quantity $dN_v(E)$ represents the number of photons emitted by the source S at energy E reaching the voxel *v*. Quantities $dp_{Ra}(E)$ and $dp_{Co}(E)$ represent the probability of a photon to be scattered in *v* in the direction of the detector element (i,j), respectively by Rayleigh and by Compton effect. Attenuation factors included in the terms $dN_v(E)$, $dp_{Ra}(E)$ and $dp_{Co}(E)$ are computed analytically with an incremental Siddon algorithm [9]. A step by step documentation on the deterministic calculation of single scattering is given in [4].

The time needed to calculate I_s^1 depends on the number of active voxels N_{vox}, the number of detector pixels $N_{\det}$, and to a less extent to the number of energy bins used to sample the x-ray spectrum. The major computational burden is dominated by the ray-tracing algorithm used to calculate the attenuation factor from one point to another. Thus, the computation time follows an affine function of $N_{vox} \times N_{\det}$. It can be consequently diminished by reducing either N_{vox} with an optimal object sampling [4] and/or by reducing $N_{\det}$. In cone-beam geometry $N_{\det}$ can be relatively high, therefore calculating Equ. 1 for each individual pixel would increase the computing time prohibitively. The Forced Detection (FD) method, originally a Monte Carlo variance reduction technique, “forces” the photons to interact with a subset of the pixels. For each voxel *v*, a number N_{FD} ($N_{FD} << N_{\det}$) of indexes are chosen randomly, and a weighting factor, $w = N_{\det} / N_{FD}$, is assigned to correct for the fact that only the forced detector pixels have been touched. The scattering estimations produced with the FD method are no longer noise-free, yet they can largely benefit from image deblurring techniques.

2.2. 3D DE-NOISING WITH THE RICHARDSON-LUCY ALGORITHM

Several deconvolution methods have been proposed to reduce these degradations, including the Richardson-Lucy (RL) iterative algorithm [10, 11], which computes the Maximum-Likelihood estimation adapted to Poisson statistics. It is being successfully used in many image restoration/resolution enhancement applications, for instance in deblurring confocal microscope imaging [12] or in de-noising scatter projections [8]. Because the inverse problem is ill-posed and the Maximum-Likelihood is nonregularized, the RL algorithm tends to amplify noise with the iterations. So to obtain a good result, the algorithm has to be stopped at early

iterations. Mathematical alternatives such as Bayesian approach [12] or generalized cross-validation as stopping rule [13] are available but with the price of an additional computation cost.

The 2-D fitting makes use of the *a priori* knowledge about the smoothness of individual scatter projections, and a Gaussian kernel with deviation σ_{xy} is chosen to describe the Point Spread Function in the detector plane. Since scatter projections tend to change slowly with the projection angle (referred as θ and N_θ being the number of angular projections), 3-D Gaussian kernels, extending in the angular direction with a deviation σ_θ, also form an accurate basis for decomposing the scatter distribution. Information from neighboring projections can now be combined during the fitting. The choice of σ_{xy} and σ_θ is an important subject because from their value depends the noise reduction and consequently the acceleration factor of the method. The acceleration stems from the fact that simulations with low number N_{FD} can effectively and rapidly be estimated by the fitting procedure.

The estimator for scatter is now calculated for all projections $\left\{\tilde{p}_{jk}\right\}_{j=1..N_{\text{det}},k\in N_\theta}$ simultaneously by blurring the virtual scatter distribution $\left\{\lambda_{jk}\right\}_{j=1..N_{\text{det}},k\in N_\theta}$ with a 3-D Gaussian function, extending both in the projection plane *k*

$$\tilde{p}_{jk}=\sum_{i\in N_j}G_{ij}^{xy}\lambda_{ik}=\frac{1}{2\pi\sigma_{xy}^2}\sum_{i\in N_j}\exp\left(-\frac{(x_i-x_j)^2}{2\sigma_{xy}^2}\right).\lambda_{ik}\qquad j\in 1...N_{\text{det}} \tag{2}$$

And at detector *j* in the angular direction

$$\tilde{p}_{jk}=\sum_{l\in N_k}G_{lk}^{z}\lambda_{jl}=\frac{1}{2\pi\sigma_\theta^2}\sum_{l\in N_k}\exp\left(-\frac{(z_l-z_k)^2}{2\sigma_\theta^2}\right).\lambda_{jl}\qquad k\in 1...N_\theta \tag{3}$$

where N_k denotes the neighbors of voxel with index k. Starting from a uniform underlying distribution, the values of $\left\{\lambda_{jk}\right\}$ are updated iteratively, according to the RL algorithm. The update for the underlying 2D *k*-th projection after *n* iterations of RL is

$$\begin{cases}\lambda_{ik}^{n+1}=\lambda_{ik}^{n}.\dfrac{\sum_{j\in N_i}G_{ij}^{xy}\left(\dfrac{\tilde{p}_{jk}}{p_{jk}^{n}}\right)}{\sum_{j\in N_i}G_{ij}^{xy}}\\ p_{jk}^{n+1}=\sum_{i\in N_j}G_{ij}^{xy}\lambda_{ik}^{n+1}\end{cases} \tag{4}$$

where the term $\left\{p^n\right\}$ is the low-noise estimate of the sought scatter projection after n iterations of 2-D RL fitting. The same procedure is then reapplied along the angular dimension by replacing the scatter distribution $\left\{\tilde{p}\right\}$ with the result of the 2D RL fitting

$\{p^n\}$, and the kernel G^{xy} with G^z. In order to determine the standard deviation of the Gaussian kernel of the fit, the balance between noise reduction and blurring of the genuine projection details has to be taken into account. Small kernels allow to model more precisely the high frequency components of the scatter distribution, but also amplify the noise during the iterations of the RL fit. They are beneficial only for fitting deterministic FD simulations based on large N_{FD}. On the other hand, larger kernels should be used to fit deterministic FD simulations with low N_{FD}. For the 2-D fitting case, [14] contains a detailed study on the choice of optimal number of iterations and optimal value of σ_{xy} depending on N_{FD} in the initial deterministic simulation.

3. *PHANTOM AND SIMULATION PARAMETERS*

A motorcycle engine in aluminium of overall dimension 18 cm^3 with 0.14 cm voxels, which correspond to an object grid of 128^3 has been used for the present simulation study. The object is illustrated in figure 1.

Fig. 1. 3D-CAD model of an Aluminium motorcycle engine cylinder

The simulations performed are intended to model an industrial cone-beam CT scanner. The CT device is equipped with a large flat CsI scintillator and a charge-coupled device (CCD). Focal length is set to 1000 mm, the distance from the source to the detector is constant and set to 1500 mm, and the active detector size is 35.34 x 52.44 cm^2. We used a point isotropic monoenergetic source of photons of 250 keV and full detector efficiency, i.e. $\varepsilon_{\text{det}}(E,\alpha,Z_{\text{det}})=E$. The RL fitting was performed with a window size of 17x17 pixels (neighbors). The parameter used to assess the precision of each simulation is the Normalized Mean Square Error (NMSE) over a region of interest of the detector. The reference intensity corresponds to the full deterministic calculation of the single scattering, i.e. by calculating the equation (1) for all the elements (i,j) of the pixelised detectors.

4. RESULTS

Three hundred twenty projections were simulated, covering 360°. The single scatter was computed with the following amount of N_{FD} : 1, 10 and 100. In addition, sixty one projections were calculated using the full deterministic method which served as the reference. The 3D RL fit was performed for each of the scatter projection data sets obtained with the different amounts of N_{FD}. Based on previous results, we choose $\sigma_{xy} = 5.5, 4, 3.2$ respectively for $N_{FD} = 1, 10, 100$, which correspond to values yielding a minimal errors in the 2D RL fit. Different values of σ_θ were studied and one iteration of the RL fit was executed. For each of the fit obtained, the NMSE with respect to the central detector line of the 61 reference projections was determined. A full deterministic simulation takes 6.6x10^4 seconds (more than 18 hours) to get a noise-free unbiaised 2D projection.

Left panel of Fig. 2 shows the evolution of the NMSE for the case $N_{FD} = 1$ as a function of the number of iterations in the 3D RL fit. The first iteration gives systematically the best result, after a divergence is observed. This is due to the ill-posed nature of the RL fitting procedure that amplifies the noise with the iterations.

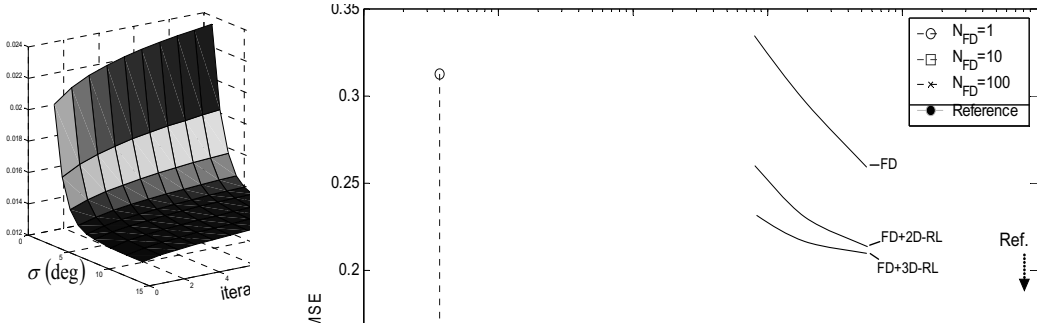

Fig. 2. Variation of NMSE in function of σ (left) and computing time vs. NMSE (right)

Middle panel of Fig. 2 shows the NMSE as a function of σ_θ(in degree). For a given number N_{FD}, the 3D RL fit give always a better result than 2D RL fit ($\sigma_\theta = 0°$). In dashed, the evolution of the optimal σ_θ (yielding minimal NMSE) for different amounts of N_{FD}. It shows that the lower the N_{FD}, the larger the optimal value of σ_θ. Since noise increases with small N_{FD}, wide Gaussian kernel become beneficial for a "good" smoothing. This behavior is comparable to what has been observed in the 2D RL fit. Right panel of Fig. 2 displays the plot of computing time versus the NMSE for the method FD alone (without RL fitting), the FD followed by 2D RL fit (noted FD+2D-RL) and FD followed by 3D RL fitting (noted FD+2D-RL). An NMSE around the percent, which we consider as a sufficient accuracy, can be achieved with $N_{FD} = 1$ in more than four orders of magnitude faster than the full deterministic simulation. Plots for a constant N_{FD} are quasi vertical, which indicate that the

computing time necessary for the RL fit is negligible with regard to the FD. The gain achieved by the 3D RL fit is mostly visible (and so beneficial) for low N_{FD}.

In Fig. 3, projections simulated with the different N_{FD} are compared. In the top-row we illustrate the primary radiation and the reference image of the single scattering obtained with the full deterministic simulation. Below, the projections computed with the FD method (without RL de-noising). Results of de-noising with 2D-RL and subsequently with the 3D-RL fit (with optimal values of the gaussian kernels) are shown on the lines below. In each case there is an obvious improvement in the fidelity of scatter estimates. Even when $N_{FD}=1$, the R-L fit allows to extract scatter distribution that closely resembles the reference.

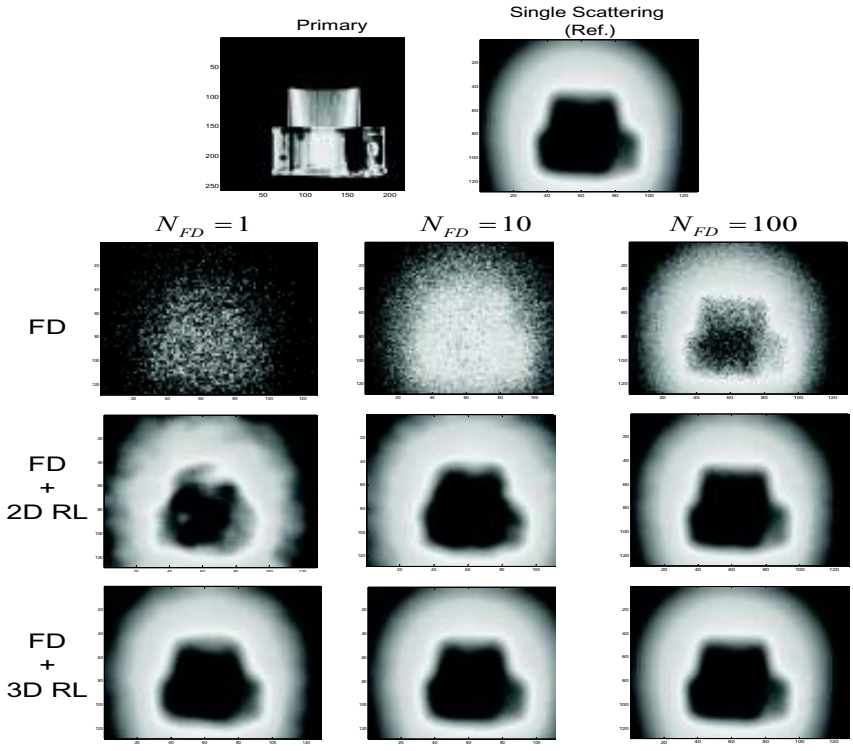

Fig. 3. Images at projection angle 72°, at various steps of the methods and with different N_{FD}

Fig. 4 compares projection profiles for the reference signal (blue line), the FD only (dashed line), and for the same FD simulation with 2D R-L fit (green line) and 3D R-L fit (red line). Already for $N_{FD}=1$ the fit of 3D-RL recovers well the genuine features

of the scatter profile from the noisy FD result. With increased N_{FD} the fine details of the reference scatter profile are recovered from the de-noised result.

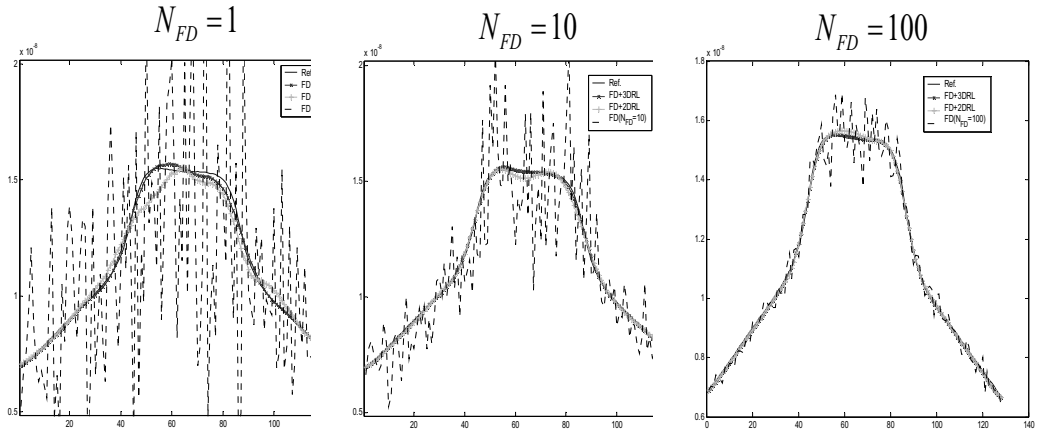

Fig. 4. Comparison of various methods with varying N_{FD} at central detector line of projection at angle 0°

5. CONCLUSION

Through this study an evidence of the efficiency of the Richardson-Lucy algorithm to de-noise results of a deterministic calculation of single scattering accelerated with the Forced Detection (FD) method is given. We showed that simulations with very few numbers of forced detectors (N_{FD}) are clearly sufficient to estimate the single scattering with a NMSE of about 1%. The RL fit is first applied with a 2D Gaussian kernel on each detector plane. Reapplying the RL fit along the angular dimension relies on the a priori smoothness of scatter distributions as a function of projection angle. The association of FD method with the 3D-RL de-noising algorithm presents an acceleration factor of the computation time by more than four orders of magnitude compared to a standard deterministic approach. Moreover, the fitting procedure yields accurate results at the very first iteration of the RL which avoid any concern about the stopping rule. The presented method achieves an exceptional compromise in term of accuracy and computing time. A complete set of 320 cone-beam single scattering projections can be computed in 20 minutes on a single 2 GHz PC and does not require tremendous memory capacity. It can be very well used for fast simulation and accurate corrective reconstruction in transmission X-ray imaging.

REFERENCES

[1] P.M. Joseph, R.D. Spital, Med. Phys. 9 (1982) 464.

[2] W. Kalender, Phys. Med. Biol. 26 (1981) 835

[3] P.C. Johns, M. Yaffe, Med. Phys. 9 (1982) 231.

[4] N. Freud. PhD Thesis , INSA-Lyon, (2003)

[5] Y. Kyriakou, T. Riedel, W.A. Kalender, Phys. Med. Biol. 51 (2006) 4567.

[6] W. Zbijewski, F. Beekman, IEEE Trans. Med. Imag. 25 (2006) 817

[7] G-R. Jaenisch, C. Bellon, U. Samadurau, S. Podoliako, M. Zhukovskiy , Eur.Conf. NDT 2006,

[8] A.P. Colijn, F.J. Beekman, IEEE Trans. Med. Imag., 23 (2004) 584.

[9] M. Christiaens, B. De Sutter, K. De Bosschere, J. Van Campenhout, and I. Lemahieu, J. Systems. Architecture, 45 (1999) 781

[10] W. Richardson, J. Opt. Soc. Amer., 62 (1972)55

[11] L. Lucy, Astronom. J., 74 (1974) 745

[12] N. Dey, L. Blanc-Feraud, C. Zimmer, P. Roux, Z. Kam, J-C. Olivo-Marin and J-Zerubia, Microscopy Research and Technique, 69 (2006) 260

[13] K. Perry, S. Reeves, The restoration of HST Images and Spectra II (1994) 97

[14] R. Thierry, A. Miceli et al NIM-A *(correction status), 2007*